Motion in Fluids Lab Report (Resubmission)

Aditya Gautam
Sen Yuan

Department of Physics, University of Toronto
PHY324: Practical Physics II

October 19, 2024

Abstract

This experiment investigates the motion of objects in fluids with high and low Reynolds numbers. By using a recording position of Teflon beads falling through glycerine (low R_e) and nylon beads falling through water (high R_e) we find the experimental Reynolds number values and compare them with the theoretical values from our calculations. Our measured and theoretical values for terminal velocity and R_e lie within 10% of each other's values. Overall, we are able to show that Reynold's number depends on the terminal velocity equations obtained from the equation for drag force for high and low R_e situations, the R_e obtained is indicative of the type of force that dominates fluid motion: viscous for low and inertial for high.

1 Introduction

Viscosity is a core factor that determines the nature of motion through a fluid, which arises from the cohesive force between particles of the fluid medium. Usually, we find inertial forces to be more dominant, but in some cases, we find that the converse holds.

We can quantify this by comparing the inertial and the viscous forces, which gives us Reynold's number for that system. The more inertial the motion is, the higher we expect the Reynold's number to be:

$$R_e = \frac{F_{inertial}}{F_{viscous}} = \frac{\rho L v}{\eta}$$

Here, ρ is the fluid medium's density, L is the characteristic length v is the flow speed, and η is the dynamic viscosity of the medium. This can be derived from the Navier-Stokes equation for an incompressible fluid.

Background Theory

This experiment aims to calculate Reynold's number for a spherical object in a fluid medium. Considering our setup explained later in this section, we need to calculate the four variables for Reynold's number in a stable scenario. Note that for a spherical body in a fluid, we take the diameter to be the characteristic length (Rhodes, 1989).

Density, viscosity, and characteristic length are all easy to measure empirically, but for the flow speed, we build upon the notion of terminal velocity. Not only is it easy to measure and analyze, but it also is a good characteristic for when the viscous and inertial forces balance out. When gravitational and drag forces reach an equilibrium, we can use the equations of motion to acquire a relation between the terminal velocity and the characteristic length of the spherical beads.

Referencing the manual (Lee & Vahabi, 2024), at the drag force equation F_d can be written as:

$$F_d = \frac{1}{2}\rho C_d A v^2 \quad \text{(for high } R_e\text{)}$$
$$F_d = 6\pi\eta r v \quad \text{(for low } R_e\text{)}$$

For the first equation, C_d is the drag coefficient of the fluid medium, ρ is the density of the fluid, and A is the cross-sectional area of the object. For the second equation, η is the (dynamic) viscosity of the medium, r is the radius of the particle in motion. In both scenarios, v is the velocity of the object.

At equilibrium, we expect $F_d = F_G = mg$, and we can solve this relation to calculate the terminal velocity equations for both scenarios:

$$v_{\text{term}} = \sqrt{\frac{2mg}{\rho C_d A}} \quad \text{(for high } R_e\text{)}$$
$$v_{\text{term}} = \frac{mg}{6\pi\eta r} \quad \text{(for low } R_e\text{)}$$

The mass of the object is calculated using relative density ($\rho_{\text{sphere}} - \rho_{\text{fluid}}$) times the volume($V$) of the object, which varies with r^3 for three dimensional objects, we have:

$$v_{\text{term}} \propto \sqrt{r} \text{ (for high } R_e\text{)} \quad \& \quad v_{\text{term}} \propto r^2 \text{ (for low } R_e\text{)}$$

We used these equations to model fitting functions for our data. The setup we use records the position of the body in the medium across time. If we plot the position vs. time data and try and fit a line to the end of this (when we expect the body to hit terminal velocity), the slope of the line should give us the terminal velocity.

One key experimental observations: a ball dropped closer to the edge faces more drag than towards the centre of the tank. This is due to the viscosity being affected by the walls and not having the same effect as falling through unbounded fluid. To account for this, we use an equation to adjust dropping a ball of diameter d in the centre of a tank of dimension D (Lommatzsch T et. al., 2001):

$$v_{\text{corr}} = v_m \frac{1}{\left(1 - 2.104\frac{d}{D} + 2.089\left(\frac{d}{D}\right)^3\right)}$$

Lastly, we used a linear fit for the position versus time data to calculate the velocity and we used a square fit and a square root fit for the plots for terminal velocity vs size, in line with the aforementioned equations for terminal velocity low and high Reynold's numbers respectively.

$$y_{\text{linear}} = mx + b \quad ; \quad y_{\text{square}} = ax^2 + b \quad ; \quad y_{\text{linear}} = a\sqrt{x} + b$$

Experimental Setup

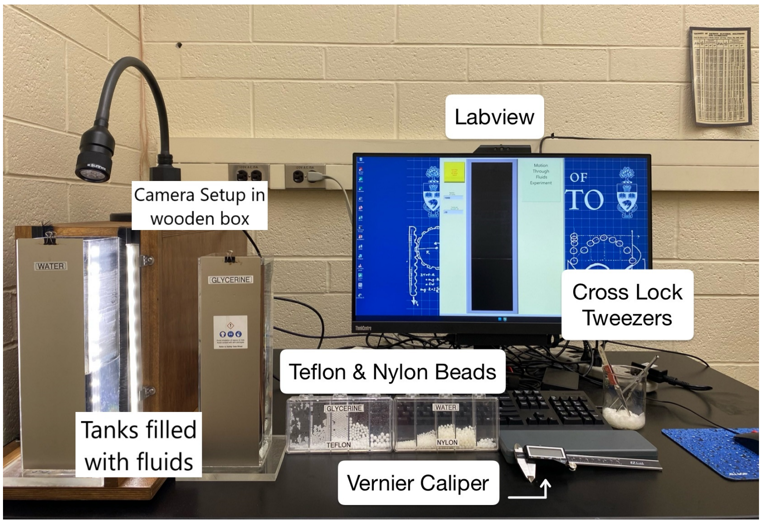

Figure 1: Experimental Setup Image from the lab manual

Our setup had two identical tanks of dimensions: $(9.3 \pm 0.1cm) \times (9.3 \pm 0.1cm) \times (32.0 \pm 0.1cm)$. Both were filled to the brim, one with distilled water and the other with pure glycerine. We used two sets of white spherical beads and took four balls for each of the five different diameters. One set of Teflon beads for measurement in glycerine and one set of nylon beads for water. We also used a fine clipper and a pair of cross-lock tweezers for dropping the beads into the liquids.

We used digital calipers (iGaging IP54) to measure the radius of the beads, Labview recording software for a camera (Chameleon 3 CM3-U3-3154M Camera) in a wooden box, and LED bulbs to detect the bead and record the data of its falling motion, We also used a web stopwatch for timing, and a Vaughan digital infrared thermometer for measuring the temperature. Data analysis and plotting were done using Python 3.11.9.

2 Methods

2.1 Data Collection

We began by measuring the dimensions of the tank(s) and the temperature of the fluid medium.

For each size of ball for each material-medium pair, we did 1 test and 3 trials for each of the two mediums in a dark room. The test was done to estimate the falling time and settings for the recording software to have the highest possible resolution and obtain as much data as possible. For each ball, we recorded the diameter using the calipers before dropping it in the respective tank and then recorded the position with time using the software across the whole tank.

The smallest size in glycerine took too long to reach the bottom (around 3 minutes, exceeding the capacity of the recording software). For this ball, we measure the last 35 seconds of its fall instead, assuming it to have reached terminal velocity.

We tried to ensure as little interference in the recordings and minimize sources of error to the best of our capabilities (more on this in the uncertainties section).

2.2 Data Analysis

Plotting the data for position vs time revealed asymptotic curves over time. As the forces are unbalanced at first, the force of drag only increases once the velocity increases. So it takes a little bit of time before the bead actually hits terminal velocity.

The data we acquired was the position vs time for the whole duration, which curved and wasn't good for a linear fit to calculate the terminal velocity.

Instead we observed the tail end of the data seemed to be quite linear. So after trial and error, we only took the last 15% of the data for the glycerol trials, and the last 50% of the data for the water trials.

As we only need the terminal velocity to calculate the Reynold's number, we took only the last fraction of the total data by trial and error that also gave us a good fit and also relatively okay chi-squared values. This did impact the χ^2 probability to be quite high, as essentially we're choosing favorable data points, however we say that it is valid in this case as this value is not the final result required, and it needs to be linear to be a good estimate for the terminal velocity. The final values were calculated by fitting a straight line to the filtered data. See plots in Appendix for visual reference.

3 Results

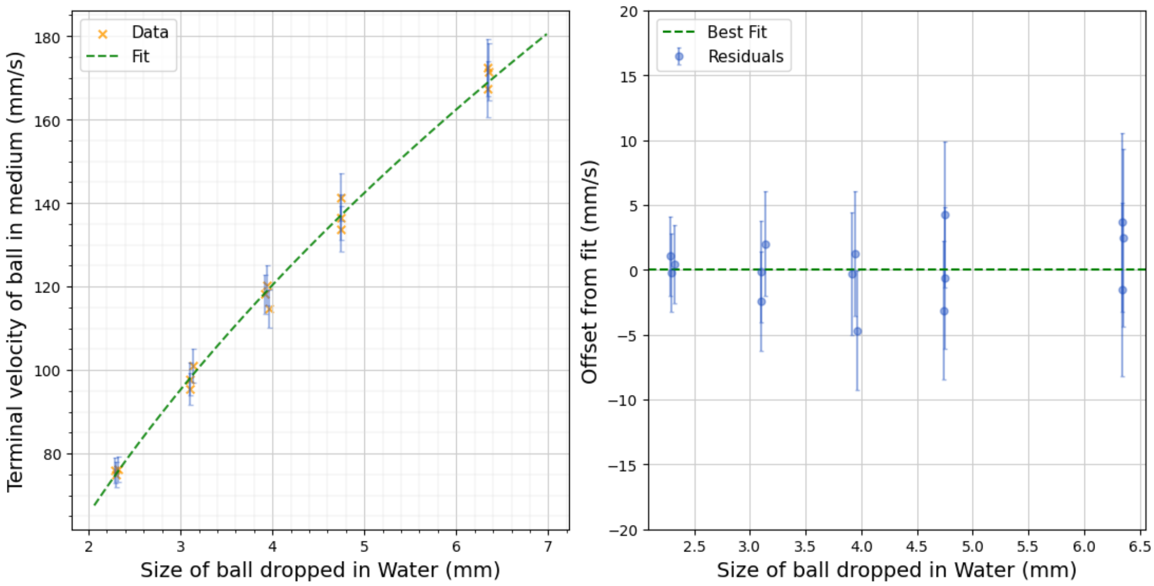

Figure 2: Graphs plotting terminal velocity as a function of bead sized dropped in water (High R_e), with residuals. The line of best fit (to last 50% of data for each trial) is a square root fit with parameters $a = 93.6 \pm 3.6$ mm$^{1/2}$s^{-1} and $b = -66.8 \pm 6.6$ mm s^{-1}. Chi-squared values are $\chi^2 = 0.65$, $\chi^2 prob = 0.72$. As the chi-sq. values and residuals are very even, we deem the fit to be very good. The residuals seem to 'fan-out' with distance, but that's due to fractional uncertainty propagating more for calculation with larger terminal velocity.

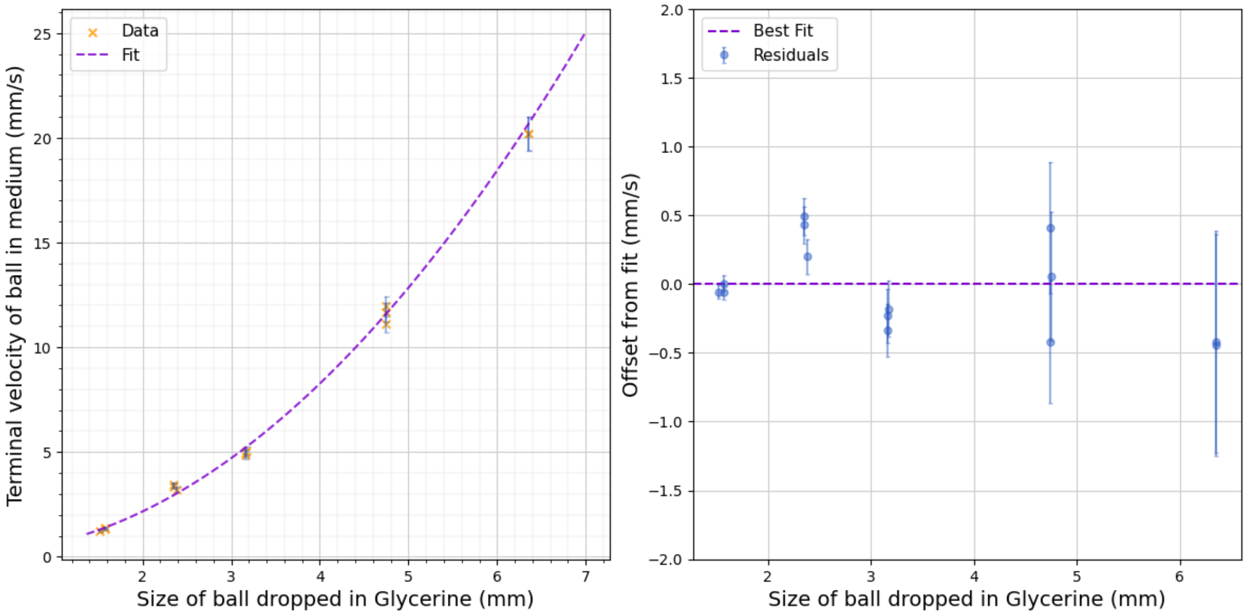

Figure 3: Graphs plotting terminal velocity as a function of bead sized dropped in glycerol (Low R_e), with residuals. The line of best fit (to last 15% of data for each trial) is a square fit with parameters $a = 0.51 \pm 0.01$ mm^{-1}s^{-1} and $b = 0.13 \pm 0.04$ mm s^{-1}. Chi-squared values are $\chi^2 = 0.25$, $\chi^2 prob = 0.88$. The chi-sq. values are decent and residuals are small, and scattered. So we deem the fit to be good. The chi-squared values are so high as the fits are to the last section of the data, which is extremely linear, and we omitted one bad data point (see uncertainties & error). As before, the residuals seem to 'fan-out' with distance, but that's due to fractional uncertainty propagating more for calculation with larger terminal velocity.

Diameter (mm)	**Measured $v_{\mathbf{term}}$ (mm/s)**	**Theoretical $v_{\mathbf{term}}$ (mm/s)**	**Measured R_e**
2.29 ± 0.01	74.9 ± 3.0	84.3 ± 4.1	180 ± 11
2.30 ± 0.01	75.8 ± 3.0	84.5 ± 4.1	181 ± 11
2.32 ± 0.01	76.1 ± 3.0	84.8 ± 4.1	184 ± 12
3.10 ± 0.01	95.5 ± 3.8	98.1 ± 4.6	310 ± 19
3.10 ± 0.01	97.8 ± 3.9	98.1 ± 4.6	317 ± 20
3.14 ± 0.01	101.0 ± 4.0	98.7 ± 4.7	332 ± 21
3.92 ± 0.01	114.7 ± 4.5	110.3 ± 5.1	475 ± 30
3.94 ± 0.01	118.2 ± 4.7	110.6 ± 5.1	484 ± 30
3.96 ± 0.01	120.2 ± 4.8	110.8 ± 5.2	495 ± 31
4.74 ± 0.01	133.8 ± 5.3	121.3 ± 5.7	663 ± 41
4.75 ± 0.01	136.5 ± 5.4	121.4 ± 5.7	678 ± 42
4.75 ± 0.01	141.4 ± 5.6	121.4 ± 5.7	702 ± 44
6.34 ± 0.01	172.5 ± 6.9	140.3 ± 6.5	1144 ± 71
6.34 ± 0.01	167.2 ± 6.6	140.3 ± 6.5	1109 ± 69
6.35 ± 0.01	171.4 ± 6.8	140.4 ± 6.5	1139 ± 70

Table 1: Showing Diameter, Theoretical Velocity, Measured Velocity, and Reynolds Number for balls dropped in water. As expected, the Reynold's number is high, of the order of magnitude 10^3. Very little disparity between measured and theoretical value, indicating a good fit.

Diameter (mm)	Measured $v_{\mathbf{term}}$ (mm/s)	Theoretical $v_{\mathbf{term}}$ (mm/s)	Measured R_e
1.52 ± 0.01	1.25 ± 0.05	1.04 ± 0.01	0.0021 ± 0.0001
1.57 ± 0.01	1.32 ± 0.05	1.11 ± 0.01	0.0023 ± 0.0001
1.57 ± 0.01	1.39 ± 0.06	1.11 ± 0.01	0.0024 ± 0.0001
2.35 ± 0.01	3.37 ± 0.13	2.49 ± 0.03	0.0088 ± 0.0005
2.35 ± 0.01	3.43 ± 0.14	2.49 ± 0.03	0.0089 ± 0.0005
2.38 ± 0.01	3.21 ± 0.13	2.55 ± 0.03	0.0085 ± 0.0004
3.16 ± 0.01	4.87 ± 0.19	4.50 ± 0.06	0.0171 ± 0.0009
3.16 ± 0.01	4.98 ± 0.20	4.50 ± 0.06	0.0174 ± 0.0009
3.17 ± 0.01	5.06 ± 0.20	4.53 ± 0.06	0.0178 ± 0.0009
4.74 ± 0.01	11.13 ± 0.45	10.12 ± 0.14	0.0585 ± 0.0027
4.74 ± 0.01	11.66 ± 0.47	10.12 ± 0.14	0.0614 ± 0.0031
4.75 ± 0.01	11.97 ± 0.48	10.17 ± 0.14	0.0629 ± 0.0031
6.35 ± 0.01	20.19 ± 0.81	18.17 ± 0.25	0.142 ± 0.007
6.35 ± 0.01	20.21 ± 0.81	18.17 ± 0.25	0.142 ± 0.007

Table 2: Showing Diameter, Theoretical Velocity, Measured Velocity, and Reynolds Number for balls dropped in glycerine. As expected, Reynold's number is very low $\sim 10^-1$ to 10^-3. Not too much disparity between measured and theoretical values. Uncertainties are too small for the smallest size, but that's partially due to the propagation method used and how we omitted 85% of the datapoints as the beads had not reached terminal velocity before then. Specifically, around size 2.35 mm, there is a large disparity from the measured velocity, possibly due to turbulence and them being the last trial.

Sources of Error and Uncertainty Calculations

For each recording, we made sure to have the lights in the room turned off and placed on the screen to avoid any see-through spots in the tank, which may cause uncertainties. We also ensured our body parts were not touching the table or setup. Lastly, we dropped the balls using the tweezers for the smaller size and clippers for the larger size just after the last beep of the software, except for the smallest Teflon balls. The balls were submerged below the surface so we could barely see the entire ball in the camera at the very top. This ensured minimum influence from the tweezers.

Our main sources of error are human errors and limitations of the setup. No setup is perfect and sources of error still exist in obtaining perfect undisturbed motion in a fluid, avoiding random spots in the camera's field due to bubbles or external light, or from the un-level base of the fluid tank from past trials. As mentioned before, we tried to minimize the error as much as possible.

Uncertainty calculation was done by propagating fractional uncertainties from the time and position uncertainties for velocity. See a sample calculation in the appendix.

For bead size, it was the least count for the calipers as seen in Tables 1 & 2.

For water: density = 0.99 ± 0.01 g/mL viscosity = 0.946 ± 0.01 centipoise calculated using a website link(1), and for glycerine: density = 1.26 ± 0.01 g/mL viscosity = 11.37 ± 0.01 poise link(2).

For position, we took the smallest delta in position for the smallest size in each medium as the least count and rounded for significant figures. For time, we took the smallest measurement of the detector and considered twice the LC reading would affect the first and last measure of the interval. We also rounded this up for uncertainty calculations.

4 Discussion

We omitted showing the Theoretical Reynold's numbers in the two tables above due to space constraints and to retain clarity. As the calculation for theoretical and measured would be the same, the only value to differ would be the terminal velocity. So the difference between the theoretical and measured R_e values would be directly proportional to the difference for the v_{term} values.

One very interesting pattern was that the difference between the measured and theoretical values only varies a lot for the beads of size $2.3mm$ mark for both mediums, which makes us wonder if there was some issue in the calculation. But As all our other terms seem to match up just fine, the plots seem reasonable, and no other issues presented themselves, we claim this to be an extrema in the equations used. The two values lie within the uncertainty regions of each other for most of the trials, so this shouldn't pose as an issue for the validity of the general experiment. One possibility could be that this particular size experiences very little wall effect due to some specific tuning/resonance of the setup, such that maybe the v_corr equation might not have been needed, which in our 'behind the scenes calculations' somewhat lines up but only for that trial. Ultimately, no setup is perfect and we're not sure what the exact source of error is.

Overall, this verifies the equations given to us. For *most* of our trials, we say what we set out to, the dominance of viscous forces over inertial forces or vice versa, depending on Reynold's number for the fluid mediums.

5 Conclusion

Our experiment with the bead-fluid pairings was a sufficient success, where we acquired the terminal velocity of spherical beads in different viscosity fluids and used them to get the medium's Reynold's numbers. As expected, the data shows us that for a high-viscosity medium, the viscous forces dominate and result in a very low Reynolds number for glycerine (of magnitude $\sim 10^{-1}$ - 10^{-3}). On the contrary, water being not very viscous, 10^{-3} times less viscosity by the magnitude of glycerine, the inertial forces dominate for fluid motion and result in a much much larger Reynold's number ($\sim 10^3 - 10^4$). Furthermore, our collected values are reasonably close (within 10% of the measurement) but lie outside of our uncertainty interval. We claim this is due to external sources of error that cannot be quantified just by the uncertainty propagation we performed.

6 References

Lee C., Vahabi T., (2024). *Motion in Fluids Lab Manual* (Revision: 63bbf38). Link

Rhodes, M. (1989). *Introduction to Particle Technology.* Wiley. ISBN 978-0-471-98482-5.

T, Lommatzsch, Megharfi, M., Mahe, E., & Devin, E. (2001). *Conceptual study of an absolute falling-ball viscometer.* Metrologia, 38(6), 531–534. https://doi.org/10.1088/0026-1394/38/6/7

Link(1) - https://www.omnicalculator.com/physics/water-viscosity

Link(2) - https://www.met.reading.ac.uk/s̃ws04cdw/viscosity_calc.html

7 Acknowledgement of AI Use

The authors of this report did not use any generative AI, LLM, or any other AI software for writing this report, except possibly the Google Docs in-built spell-check tool.

Appendix

Reasoning for Partial fit instead of Full fit for dataset

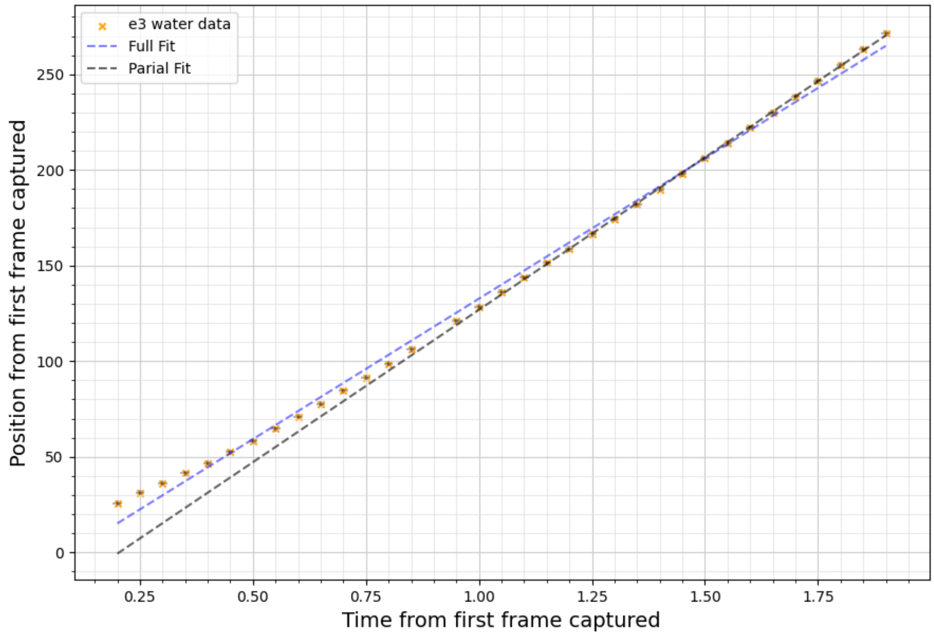

Figure 4: Graph showing full fit (B=blue) versus partial fit (black) for nylon balls in water data (orange crosses). Values omitted. E3 indicates trial of the largest size, which was chosen to show good curvature.

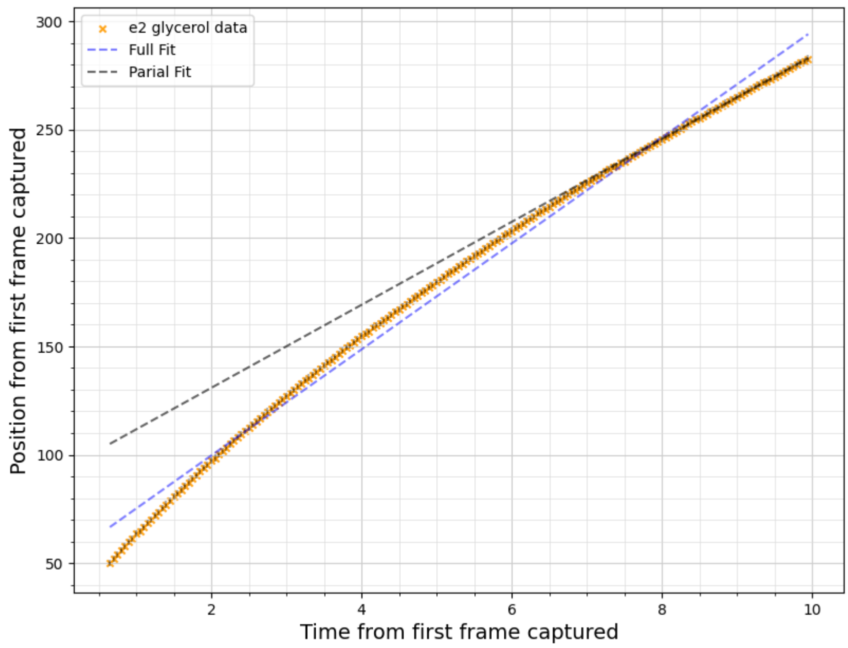

Figure 5: Graph showing full fit (blue) vs. partial fit (black) for Teflon beads in glycerine data (orange crosses). Values omitted. E2 indicates second trial of the largest size, which was chosen to show good curvature.

Uncertainty Calculations:

We sample the calculations for teflon in glycerine at diameter 4.74 mm (1st trial)

Glycerine:

$\Delta t/t = 0.02$ (Calculated as sum of uncertainties)

$\Delta x/x = 0.02$ (d.o.)

$\Delta v/v = \frac{\Delta t}{t} + \frac{\Delta x}{x} = 0.04$

Slope of line of best fit $= v_{\text{term}} = 11.13\ \ mm/s$ (Rounded Up)

$\Delta v = 11.13 * 0.04 = 0.45\ \ mm/s$ (Rounded Up)

$\rho_{gly} = 1.26 \pm 0.01 * 10^3\ \ (\text{g mm}^{-3})$ link(2)

$\eta_{gly} = 1.137 \pm 0.001\ \ (\text{g mm}^{-1}\ \text{s}^{-1})$ link(2)

$L = d = 4.74 \pm 0.01 mm$

$$
\begin{aligned}
R_e &= \rho * L * v/\eta \\
&= (1.26 * 4.74 * 11.13/1.137) * 10^{-3} \\
&= 66.4728/1137 = 0.05846 \\
&= 0.0585 && \text{(rounded up)}
\end{aligned}
$$

$\Delta\rho/\rho = 1/126$

$\Delta\eta/\eta = 1/1137$

$\Delta L/L = 1/474$

$\Delta R_e/R_e = \frac{\Delta\rho}{\rho} + \frac{\Delta L}{L} + \frac{\Delta v}{v} + \frac{\Delta\eta}{\eta} = 1/126 + 1/1137 + 1/474 + 0.45 =\sim 0.46$

$\Delta R_e = 0.46 * 0.0585 = 0.0027$ (rounded up)

$v_{\text{theoretical}} = v_t = mg/(6\pi\eta r)$

$$
\begin{aligned}
m &= (\rho_{tef} - \rho_{gly}) * (4/3 * \pi * r^3) \\
&= (2.2 - 1.26) * 10^{-3} * 55.76139 = 52.41571 * 10^{-3}
\end{aligned}
$$

$\Delta m = m * \left(\frac{\Delta\rho}{\rho} + \frac{\Delta V}{V}\right) = 52.415 * (0.01/0.94) * 10^{-3}$ V delta negligible as $\Delta r^3 = 10^{-6}$

$g = 9.81 m/s^2 = 9.81 * 10^3 mm/s^2$

$\pi = 3.14$

$\eta_{gly} = 1.137 \pm 0.001\ \ (\text{g mm}^{-1}\ \text{s}^{-1})$

$$
\begin{aligned}
v_t &= m * g/(6 * \pi * \eta * r) \\
&= 52.4157 * 9.81/(6 * 3.14 * 1.137 * 2.37) && \text{powers of ten cancel out to zero} \\
&= 10.12
\end{aligned}
$$

$\Delta v_t = v_t * (\frac{\Delta}{} + \frac{\Delta\eta}{\eta} + \frac{\Delta r}{r})$

$\Delta v_t = v_t * (1/94 + 1/1137 + 1/474) = 10.12 * 0.0136 = 0.14$